Design optimization of flexible piezoelectric PVDF unimorphs for surface pressure transducer applications

Arun K. Ramanathan, Leon M. Headings, Marcelo J. Dapino

Arun K. Ramanathan, Leon M. Headings, Marcelo J. Dapino, "Design optimization of flexible piezoelectric PVDF unimorphs for surface pressure transducer applications," Proc. SPIE 10973, Smart Structures and NDE for Energy Systems and Industry 4.0, 1097307 (18 March 2019); doi: 10.1117/12.2514371

SPIE.

Event: SPIE Smart Structures + Nondestructive Evaluation, 2019, Denver, Colorado, United States

Design optimization of flexible piezoelectric PVDF unimorphs for surface pressure transducer applications

Arun K. Ramanathan, Leon M. Headings, and Marcelo J. Dapino*

NSF IUCRC on Smart Vehicle Concepts Department of Mechanical and Aerospace Engineering, The Ohio State University, Columbus, OH 43210

ABSTRACT

Piezoelectric elements serve as a preferred candidate for measuring dynamic pressure owing to their high sensitivity, signal-to-noise ratio, high natural frequency, and suitability for miniaturization. Polyvinylidene fluoride (PVDF) is a mechanically tough, flexible, low density polymer commercially available as a film. Being mechanically compliant and minimally invasive to the host structure, PVDF can be conformed to a variety of surfaces using adhesive bonding, thus making it a suitable candidate for surface pressure mapping and acoustic pressure measurement applications. However, PVDF sensors in compressive mode are insufficient for the low frequency and high sensitivity requirements of vehicle surface pressure measurements. Under steady flow conditions, cantilever and clamped-clamped unimorphs with segmented electrode coverage configurations serve as alternative candidates for differential pressure measurements. This paper presents an analytical and computational design framework for optimizing the performance of PVDF unimorphs. Electrode coverage, thickness ratio, and elastic modulus ratio are optimized for cantilever and clamped-clamped configurations for a given sensor geometry. The goal of the optimization procedure is to maximize charge sensitivity of the pressure sensor while minimizing deflection. A closed-form solution is derived for deflection and charge sensitivity of cantilever and clamped-clamped configurations based on Euler-Bernoulli beam theory. For a given deflection sensitivity target and sensor geometry, the charge sensitivity of the optimized cantilever sensor is three orders of magnitude greater than compressive (d_{33} mode) design and 3.15 times higher than the clamped-clamped configuration with segmented electrodes.

Keywords: piezoelectric PVDF, design optimization, surface pressure transducer, multiphysics FEM model

1. INTRODUCTION

In the field of experimental aerodynamics, pressure sensors that can simultaneously exhibit high temporal and spatial resolution are required. Conventional pressure transducers require time-consuming fixturing which renders the tested parts unusable after measurements.[1–3] In addition, the measuring holes made for mounting these transducers contribute to measurement noise. Relatively new measurement techniques, such as pressure-sensitive paint (PSP) can provide a global map of surface pressure with high spatial resolution.[4] However, the PSP technology is limited by its slower response time, low signal-to-noise ratio, and requirement of visual recorders and image processing systems.

PVDF is a flexible, low density polymer manufactured as thin sheets with thicknesses ranging from 9 µm to 100 µm. Due to their high piezoelectric constant and possibility to operate without complicated circuitry, PVDF is a promising alternative to conventional pressure and aeroacoustic transducers. Their relatively low cost and flexibility facilitate their embedment onto the surface of the structure for flow investigations. Charge amplifiers are typically used to enable a voltage readout of the charge generated by the sensor in response to applied pressure. The lower cutoff frequency of the charge amplifier is determined by its feedback capacitance and resistance. However, for a given lower cutoff frequency, the maximum attainable voltage gain of the charge amplifier is limited.[5] Therefore, in order to enable low frequency measurements, the charge sensitivity, defined as the charge output per unit applied pressure, has to be maximized.

*Further author information: (Send correspondence to M.J.D.)
A.K.R.: E-mail: ramanathan.38@osu.edu
L.M.H.: E-mail: headings.4@osu.edu
M.J.D.: E-mail: dapino.1@osu.edu

Smart Structures and NDE for Energy Systems and Industry 4.0, edited by Norbert G. Meyendorf, Kerrie Gath, Christopher Niezrecki, Proc. of SPIE Vol. 10973, 1097307 · © 2019
SPIE · CCC code: 0277-786X/19/$18 · doi: 10.1117/12.2514371

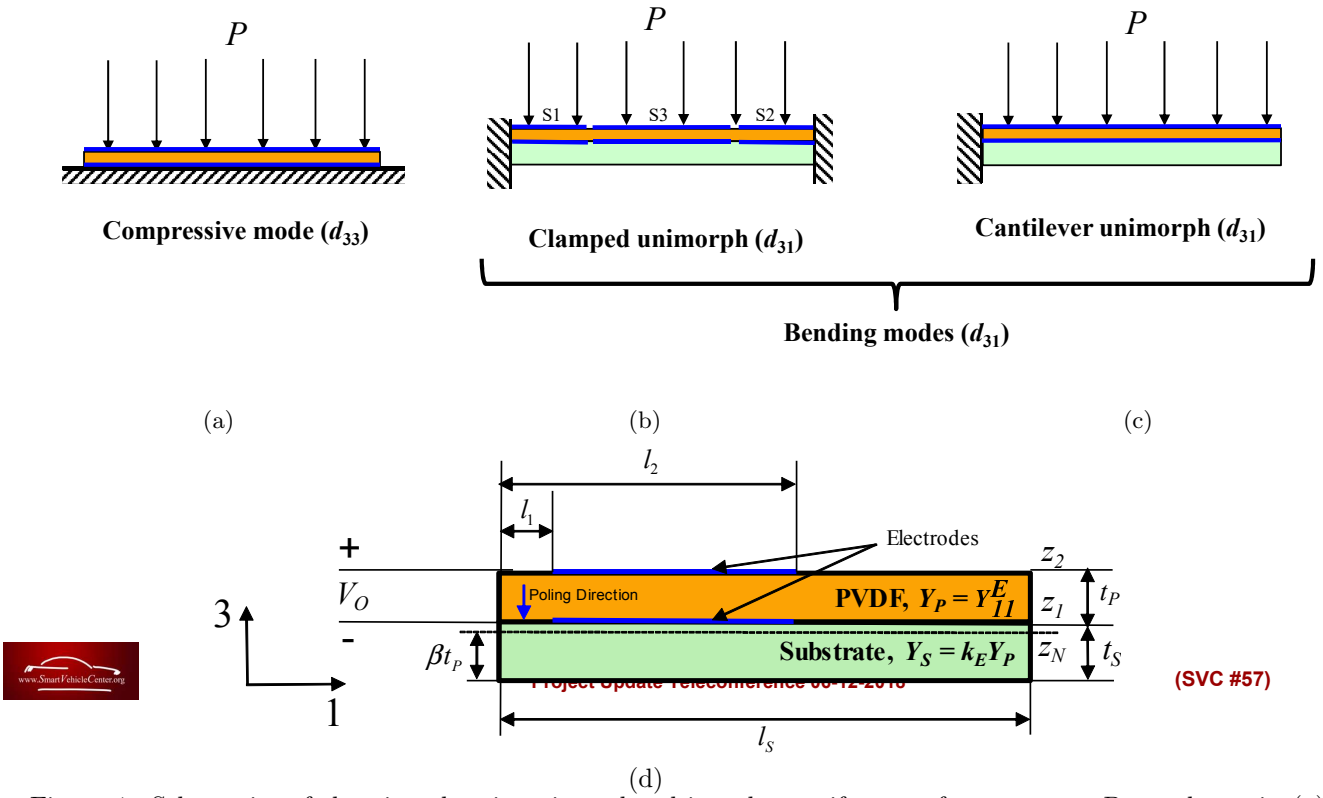

Figure 1: Schematics of the piezoelectric unimorph subjected to uniform surface pressure P are shown in (a) compressive mode, (b) clamped-clamped mode with segmented electrodes, and (c) cantilever bending mode. (d) Schematic of a piezoelectric PVDF unimorph defined by basic variables: thicknesses of the PVDF layer and the substrate are t_P and t_S, respectively, and elastic moduli for the PVDF layer under constant electric field substrate along direction 1 are Y_P and Y_S, respectively. The length of the unimorph is l_S and the electrode is covered over a length $l_2 - l_1$. The neutral axis of the structure is located at βt_P from the bottom of the substrate.

Piezoelectric sensors respond to applied pressure under compression (d_{33} mode) and bending (d_{31} mode). PVDF sensors have been successfully utilized in their d_{33} mode as a means of measuring unsteady surface pressures in aircraft wind tunnels,[6,7] marine applications,[8] and pressure impulse measurements.[9] However, the above applications are largely limited to high frequency measurements ($>$ 50 Hz) and the applied pressures are on the order of several kilopascals. Automotive aerodynamic measurements require surface pressure sensors capable of low frequency (<50 Hz) and low differential pressure measurements that range from -2 kPa to 2 kPa with a minimum response time of 1 millisecond.[10] Also, to facilitate improved spatial resolution, the dimension of the sensor is limited to a size of 5 mm x 5 mm. A PVDF sensor in d_{33} mode, shown in Figure 1(a), provides a charge sensitivity of 0.84 fC Pa^{-1} ($Q_P = d_{33}A$), which is insufficient for low frequency and high sensitivity requirements. Therefore, other sensor designs are investigated in order to maximize charge sensitivity.

Under steady flow conditions, cantilever[11] and clamped-clamped unimorphs with segmented electrode coverage[12,13] serve as alternative configurations for differential pressure measurements using PVDF. However, piezoelectric sensors operating in bending mode require a substrate in order to have a non-zero charge output. Figure 1(b) and 1(c) show the schematic of cantilever and clamped-clamped bending unimorphs. The constitutive equations for a piezoelectric unimorph under static conditions suggest that there exists a non-monotonic relationship between thickness and elastic modulus ratios of the PVDF layer to the substrate and charge sensitivity.[14] Also, in order to preserve the noninvasive nature of the pressure sensor, it is required to keep the overall dimensions of the sensor to a minimum. Therefore, the allowable deflection sensitivity, defined as the deflection per unit pres-

sure, is limited to 0.5 μm Pa^{-1} such that at maximum compressive pressure of 2 kPa, the maximum deflection of the sensor is limited to 1 mm. In this work, we present an analytical and computational design framework for optimizing the performance of PVDF surface pressure sensors for a given sensor geometry. Electrode coverage, thickness ratio, and elastic modulus ratio are optimized for cantilever and clamped-clamped configurations and compared with the compressive mode. A closed-form solution for deflection and charge sensitivity is derived for deflection and charge sensitivity of the bending modes based on Euler-Bernoulli beam theory. Using the minimum bending stiffness values required in order to achieve a deflection sensitivity target of 0.5 μm Pa^{-1}, the optimum elastic modulus and thickness ratio of the substrate for a given sensor dimensions are computed and compared against COMSOL Multiphysics®simulations.

2. ANALYTICAL MODELING OF PIEZOELECTRIC BENDING UNIMORPHS

Consider a piezoelectric PVDF unimorph beam as shown in Figure 1(a). The overall length and width of the structure is given by l and b, respectively. The thickness of the PVDF layer and the substrate is given by t_S and t_P, respectively. The elastic modulus in direction 1 for the PVDF layer under constant electric field is $Y_{11}^E = Y_P$ and the elastic modulus of the substrate is Y_S. The thickness ratio of the structure is defined as $k_t = t_S/t_P$ and the elastic modulus ratio of the structure is defined as $k_E = Y_S/Y_P$. The piezoelectric material is placed on the substrate such that the polarization due to bending deformation is same as the dielectric polarization. It is assumed that the charge generated by the piezoelectric layer is predominantly due to longitudinal stress T_1 and the contribution to charge output due to lateral stress T_2 is neglected due to a smaller d_{32} coefficient.[15] Based on classical laminate theory, it is further assumed that any line perpendicular to the neutral axis before deformation remains perpendicular after deformation, resulting in a strain that varies linearly through the thickness of the beam.[16] For planar strain conditions of a piezoelectric PVDF film, the normal strain in direction 3 and the shear strains in directions 1-3 and 2-3 are zero. Using the above approximations, the piezoelectric constitutive equations under quasi-static conditions are reduced to

$$S_{1p}(x,z) = s_{11}^E T_{1p}(x,z) + d_{31} E_3(x,z), \tag{1}$$

$$D_3(x,z) = d_{31} T_{1p}(x,z) + \epsilon_{33} E_3(x,z), \tag{2}$$

where S_{1p} and T_{1p} are the strain and stress in the piezoelectric layer, respectively; E_3 and D_3 are the electric field and polarization along direction 3; s_{11}^E corresponds to the compliance of PVDF along direction 1 and is given by the inverse of its elastic modulus; d_{31} is the piezoelectric charge coefficient and ϵ_{33}^T is the dielectric constant of PVDF at constant stress.

2.1 Generalized expression for deflection and polarization

While the piezoelectric unimorph beam is subjected to uniform surface pressure P under quasi-static conditions, the bending moment M about the neutral axis for any given point x along the length of the beam is

$$\frac{\partial^2 M(x)}{\partial x^2} = bP(x), \tag{3}$$

where b is the width of the unimorph. Typically, for structures where the piezoelectric layer is much thinner than the substrate, the bending moment is calculated about the neutral axis of the substrate.[17] However, in this case, the thickness and the bending stiffness of the PVDF layer is not negligible. Therefore, the bending moment about the neutral axis is given by

$$M(x) = -\int_0^{z_N} z T_{1s}(x,z) b dz - \int_{z_N}^{z_1} T_{1s} b dz - \int_{z_1}^{z_2} T_{1p}(x,z) b dz. \tag{4}$$

The distance from the bottom of the substrate to the neutral axis z_N is represented by[18]

$$\beta t_P = -\frac{1}{2}\left\{\frac{k_t^2 k_E + 2k_t(1-k_{31}^2) + (1-k_{31}^2)}{k_t k_E + (1-k_{31}^2)}\right\} \tag{5}$$

where k_{31} is the electromechanical coupling factor of the piezoelectric layer. The effect of elastic modulus of the substrate Y_S on βt_P is significant for compliant substrates and approaches the value of -0.5t_S with increase in elastic modulus or thickness of the substrate. For PVDF, the value of k_{31} could be as large as 0.2 and therefore not negligible.[15] Using Euler-Bernoulli theory, the strain-displacement relations in the piezoelectric layer and the substrate are expressed as

$$S_{1p}(x,z) = -z\frac{\partial^2 w(x)}{\partial x^2}, \tag{6}$$

$$S_{1s}(x,z) = -z\frac{\partial^2 w(x)}{\partial x^2}. \tag{7}$$

Using (6) in (1) and substituting $s_{11}^E = 1/Y_P$ one obtains the stress in the piezoelectric layer and the substrate as

$$T_{1p}(x,z) = -zY_P\frac{\partial^2 w(x)}{\partial x^2} - Y_P d_{31} E_3(x,z), \tag{8}$$

$$T_{1s}(x,z) = -zY_S\frac{\partial^2 w(x)}{\partial x^2}. \tag{9}$$

The bending moment about the neutral axis is obtained by using (8) and (9) in (4) and integrating through the thickness of the structure as

$$M(x) = \overline{YI}\frac{\partial^2 w(x)}{\partial x^2}, \tag{10}$$

where,

$$\overline{YI} = \frac{Y_P b t_P^3}{3}\left[k_E k_t\left(k_t^2 + 3\beta k_t + 3\beta^2\right) + \frac{1}{1-k_{31}^2}\left\{\left(1 - \frac{3k_{31}^2}{4}\right) + 3\left(1-k_{31}^2\right)\left(k_t^2 + \beta^2 + 2\beta k_t + k_t + \beta\right)\right\}\right]$$

is the bending stiffness of the piezoelectric unimorph.

The generalized displacement $w(x)$ of the piezoelectric unimorph along the length of the beam is related to the applied pressure $P(x)$ as

$$\overline{YI}\frac{\partial^4 w(x)}{\partial x^4} = bP(x). \tag{11}$$

Integrating the above equation, one obtains

$$w(x) = \frac{bP(x)}{24\overline{YI}}x^4 + \frac{c_1}{6}x^3 + \frac{c_2}{3}x^2 + \frac{c_3}{x} + c_4. \tag{12}$$

Using (8) in (2) and neglecting piezoelectric electric coupling, i.e., $E_3 = 0$, one obtains

$$D_3(x,z) = -zd_{31}Y_P\frac{\partial^2 w(x)}{\partial x^2}. \tag{13}$$

The electrodes are equipotential surfaces located at z_1 and z_2 in Figure 1(d). Using (6) in (13) for polarization along the length of the electrode is obtained by integrating the above equation through the thickness of the PVDF layer,

$$D_3(x) = -d_{31}Y_P t_P\left(\frac{1}{2} + k_t + \beta\right)\frac{\partial^2 w(x)}{\partial x^2}. \tag{14}$$

It can be observed that the polarization is proportional to the average stress along the length of the beam. The total charge output of the piezoelectric layer with an electrode coverage from l_1 to l_2 is given by integrating (14)) over the surface area A of the electrode,

$$Q = -d_{31}Y_P t_P\left(\frac{1}{2} + k_t + \beta\right)\iint_A \frac{\partial^2 w(x)}{\partial x^2}dxdy = -d_{31}bY_P t_P\left(\frac{1}{2} + k_t + \beta\right)\left[\frac{\partial w(x)}{\partial x}\right]_{l_1}^{l_2}. \tag{15}$$

It can be observed from (14) that the polarization is proportional to the average stress along the length of the beam and the corresponding charge output (15) is proportional to the difference between the slopes at the end

points of the electrode. Finally, the open circuit voltage of the sensor is given by the charge-voltage relationship as

$$V_O = -\frac{d_{31} Y_P t_P^2 \left(0.5 + k_t + \beta\right)}{\epsilon_{33}(l_2 - l_1)} \left[\frac{\partial w(x)}{\partial x}\right]_{l_1}^{l_2}. \tag{16}$$

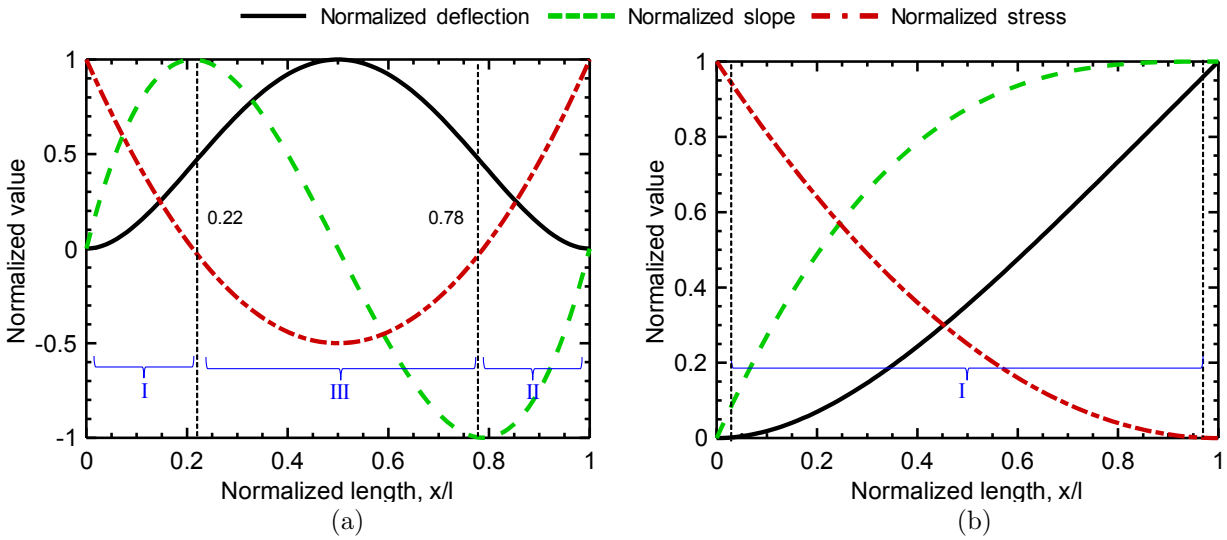

Figure 2: Normalized deflection, stress distribution, and absolute charge output along the length of the PVDF sensor in (a) clamped-clamped and (b) cantilever unimorph.

2.2 Clamped-clamped unimorph

Using Dirichlet boundary conditions, the displacement and slope at the clamped ends can be set as $w(0) = 0$, $w'(0) = 0$, $w(l) = 0$, and $w'(l) = 0$ in (11) to obtain

$$w_{clamped}(x) = \frac{bx^2(l-x)^2}{24\overline{YI}} P. \tag{17}$$

Thus, the deflection sensitivity $\delta_{clamped}$ of the unimorph given by the maximum displacement per unit applied pressure as

$$\delta_{clamped} = \frac{w_{clamped,max}}{P} = \frac{bl^4}{384\overline{YI}}. \tag{18}$$

Figure 2(a) shows the normalized deflection, slope, and stress profile along the length of the clamped-clamped beam operating below its fundamental frequency. Since the charge output is proportional to the difference between the slopes evaluated at the end points of the electrode, if a single electrode covers the entire length of the PVDF layer, the difference between the slopes evaluated at its end points, $w'(l_1 = 0) - w'(l_2 = l)$ equals zero. Therefore, the total charge output is also zero. This necessitates segmenting the electrode along the length of the sensor, such that the charge output is maximized.[13] It can be observed that the difference between the slopes is maximum if the electrodes are segmented from 0 to $0.22l$, $0.78l$ to l, and $0.22l$ to $0.78l$. The above segments are shown as I, II, and III, respectively in Figure 2(a). The difference between the slopes evaluated at the end points of segment I and II is positive, while the difference between the slopes evaluated at the end points of segment III is negative. Thus, reversing the polarity of the electrode in segment III and then assembling the three charge sources maximizes the net charge output. In other words, the electrodes have to be segmented such that there is no change in the sign of stress within that segment. In this case, it can be seen that the sensor is under tensile stress from 0 to $0.22l$ and from $0.78l$ to l, while the longer middle segment from $0.22l$ to $0.78l$ is under compression. Therefore, the net charge output due to the segmented electrodes is given by

$$Q_{clamped} = -d_{31} b Y_P t_P \left(\frac{1}{2} + k_t + \beta\right) \left\{ \left[\frac{\partial w(x)}{\partial x}\right]_0^{0.22l} - \left[\frac{\partial w(x)}{\partial x}\right]_{0.22l}^{0.78l} + \left[\frac{\partial w(x)}{\partial x}\right]_{0.78l}^{l} \right\}. \tag{19}$$

Using equation (17), under quasi-static conditions, the closed-form solution for charge sensitivity of a clamped-clamped unimorph defined as charge output per unit applied pressure is given by

$$Q_P = -\frac{0.032 d_{31} b^2 Y_P t_P l^3}{\overline{YI}} \left(\frac{1}{2} + k_t + \beta \right). \tag{20}$$

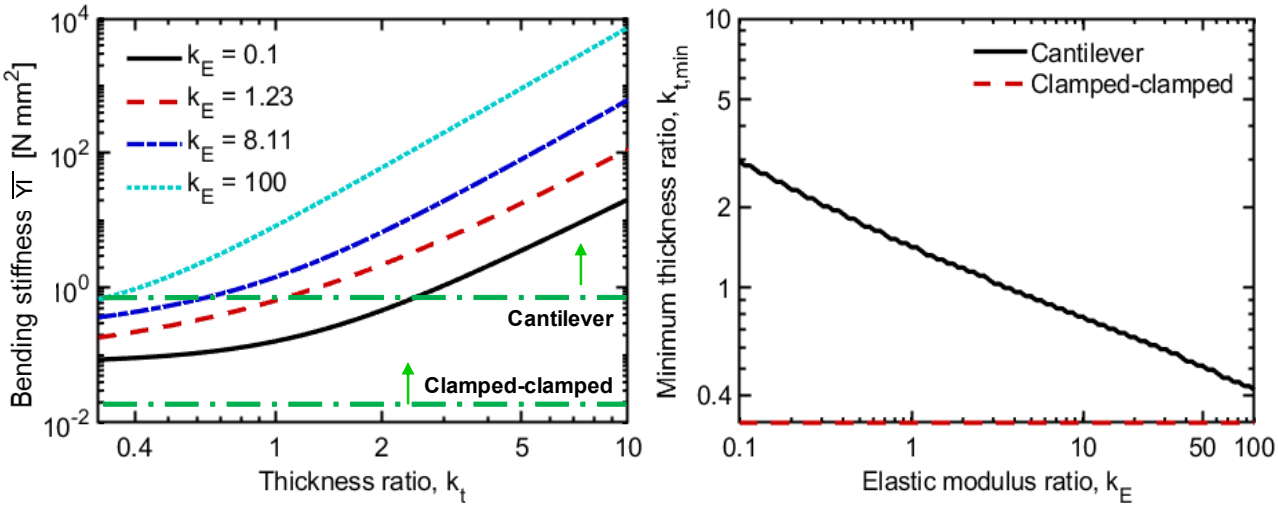

(a) (b)

Figure 3: Calculated k_t vs $\overline{YI}$ of the unimorph for different k_E values. The arrows indicate the feasible region for the unimorph configuration for maximizing charge sensitivity, (b) minimum k_t for achieving deflection sensitivity target of 0.5 μm Pa^{-1} for different k_E values.

2.3 Cantilever unimorph

Using Dirichlet boundary conditions, the displacement and slope at the clamped and free ends can be set as $w(0) = 0$, $w'(0) = 0$, $w''(l) = 0$, and $w'''(l) = 0$ in (11) to obtain

$$w_{cantilever}(x) = \frac{bx^2(6l^2 - 4lx + x^2)}{24\overline{YI}} P. \tag{21}$$

Thus, the deflection sensitivity $\delta_{clamped}$ of the unimorph given by the maximum displacement per unit applied pressure as

$$\delta_{cantilever} = \frac{w_{cantilever,max}}{P} = \frac{bl^4}{8\overline{YI}}. \tag{22}$$

When the cantilever operates below its first bending mode, the stress is higher near the clamped end and very low near the free end of the beam and there is no change in direction due to deflection as shown in 2(b) Also, the slope of the beam increases from zero and it is maximum at the free end. Therefore, electrodes covering the entire length of the beam would provide the maximum charge output. Utilizing (21) in (12), the net charge output of a cantilever beam is given by

$$Q_{cantilever} = -d_{31} b Y_P t_P \left(\frac{1}{2} + k_t + \beta \right) \left[\frac{\partial w(x)}{\partial x} \right]_0^l. \tag{23}$$

Finally, the charge sensitivity of the cantilever unimorph is

$$Q_P = -\frac{0.167 d_{31} b^2 Y_P t_P l^3}{\overline{YI}} \left(\frac{1}{2} + k_t + \beta \right). \tag{24}$$

From (20) and (24), it can be observed that for small deflections, the deflection sensitivity of the cantilever is 48 times greater than for the clamped-clamped beam, whereas the charge sensitivity of the cantilever is 5.2 times greater than for the clamped-clamped beam with segmented electrode coverage.

Table 1: PVDF pressure sensor properties. The subscripts S and P refer to substrate and the PVDF sensor, respectively.

Geometric parameters		**Material properties of PVDF film**	
Length x width of the substrate, l x w	5 x 5 [mm^2]	Young's modulus of PVDF film, Y_P	2.74 [GPa]
Length x width x thickness of the PVDF film, l x w x t_S	5 x 5 x 0.040 [mm^3]	Poisson's ratio of PVDF film, ν_P	0.39
Material properties of the substrate		Piezoelectric charge coefficient of PVDF film in direction 1, d_{31}	23.58 [pC N^{-1}]
		Piezoelectric charge coefficient of PVDF film in direction 1, d_{32}	3.48 [pC N^{-1}]
Density of the host structure, Y_S	1200 [kg m^{-3}]	Piezoelectric charge coefficient of PVDF film in direction 1, d_33	-33.8 [pC N^{-1}]
Poisson's ratio of the host structure, ν_S	0.3	Dielectric constant of PVDF film in direction 3, ϵ_{33}	68.5 [pF m^{-1}]

3. NUMERICAL SIMULATION AND DISCUSSION

Finite element modeling (FEM) of the piezoelectric unimorph is performed using COMSOL Multiphysics to arrive at optimal substrate properties – thickness and elastic modulus of the substrate for maximum charge sensitivity for the allowed deflection sensitivity. The contribution of d_{32} and d_{33} on charge sensitivity is also investigated. The geometric and material property values assigned for PVDF and the substrate are given in Table 1. The substrate material is assumed to be isotropic and electrically non-conductive. In consideration with material availability and fabrication feasibility, the investigated region for optimization of k_t is from 0.3 to 10 and for optimization of k_E is from 0.1 to 100. The elastic compliance, permittivity, and the piezoelectric coupling tensor utilized for PVDF material in the FEM model can be found elsewhere.[19]

In order to keep the overall thickness of the sensor at a minimum, the deflection sensitivity of the sensor is limited to 0.5 μm Pa^{-1} so that a pressure input of 2 kPa would produce a total deflection of 1 mm. Using the relations (18) and (22) and using the values in Table 1, minimum bending stiffness for clamped-clamped and cantilever unimorphs are given by

$$\overline{YI}_{min,clamped} = \frac{bl^4}{384\delta_{clamped}} = 0.0163 \text{ Nmm}^2, \text{and} \tag{25}$$

$$\overline{YI}_{min,cantilever} = \frac{bl^4}{8\delta_{cantilever}} = 0.7813 \text{ Nmm}^2. \tag{26}$$

Since the bending stiffness of the structure exhibits a coupling of k_t and k_E, it is solved numerically from a discrete set of k_t and k_E values. Figure 3(a) shows the bending stiffness as a function of k_t for different k_E values. Within the investigated range, the clamped-clamped configuration meets the bending stiffness target for all k_t and k_E values, whereas the cantilever configuration has a minimum k_t for each k_E. Figure 3(b) shows the minimum thickness ratio $k_{t,min}$ computed for each k_E. It can be seen that $k_{t,min}$ decreases almost linearly on a logarithmic scale with increase in k_E. The optimum substrate thickness and elastic modulus ratio for maximum charge sensitivity should meet these k_E and $k_{t,min}$ values.

Figure 4(a) and (c) show the deflected shape and the longitudinal stress distribution across the PVDF layer for the clamped-clamped structure and cantilever. As described by the analytical model, the clamped-clamped configuration shows maximum tensile stress at its clamped ends, while its longer middle segment is under compression. However, with segmented electrode coverage, the magnitude of charge sensitivity is computed for each of the segment shown by the solid lines and added up. For the cantilever unimorph, PVDF layer is under tension throughout the length of the beam. Using (20) and (24), the charge sensitivities of the unimorphs are calculated for the set of k_t and k_E values that satisfies the bending stiffness target and compared with the FEM.

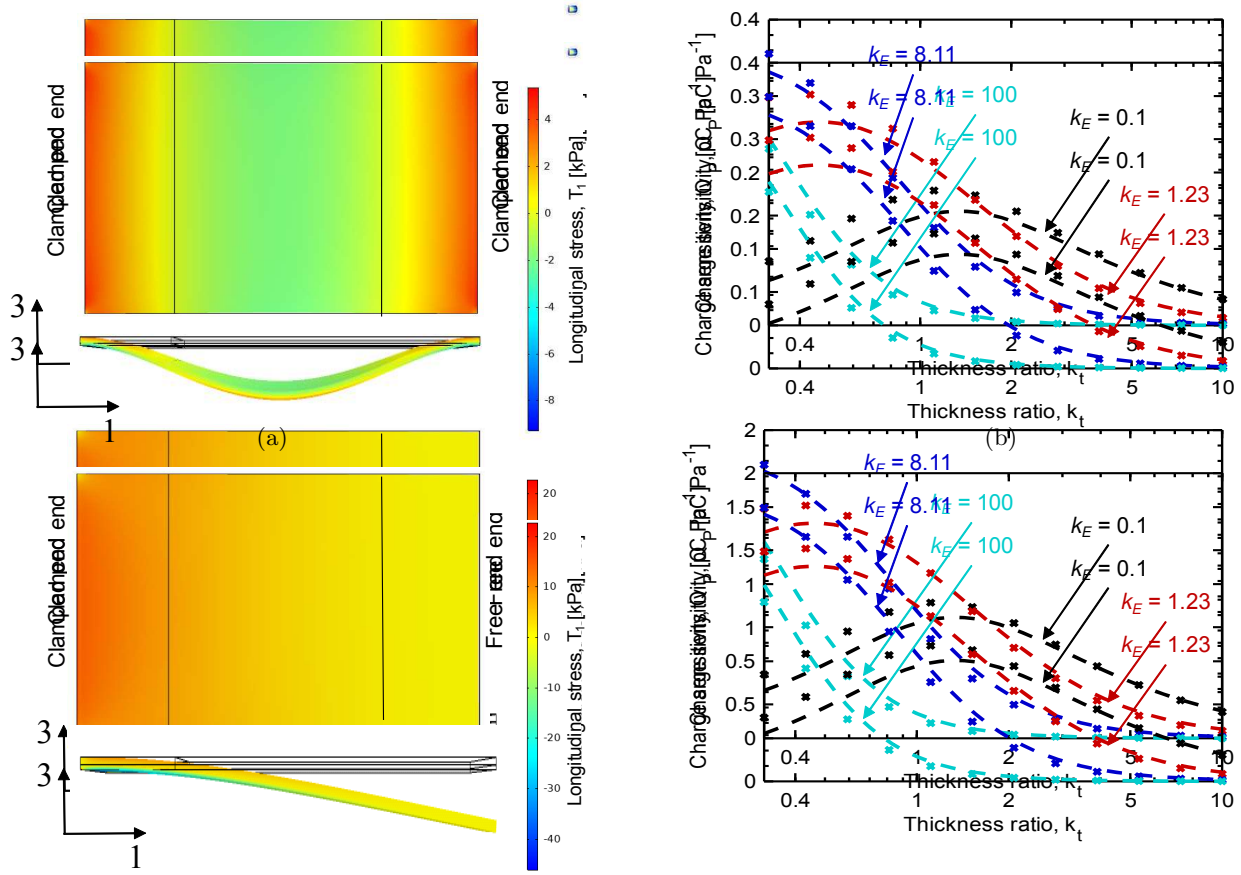

Figure 4: (a) FEM results of T_1 when the clamped-clamped unimorph is subjected to uniform pressure $P = 1$ Pa for $k_E = 8.11$ and $k_t = 0.32$, (b) analytical (solid lines) and FEM (markers) of charge sensitivity as a function of k_t for different k_E values for clamped-clamped, (c) FEM results of T_1 when the cantilever unimorph is subjected to uniform pressure $P = 1$ Pa for $k_E = 0.81$, (d) analytical (solid lines) and FEM (markers) of charge sensitivity as a function of k_t for different k_E values for cantilever.

Figure 4(b) and (d) shows that theory generally agrees well with the FEM simulation. It can also be observed that k_t versus Q_P exhibits a peak and the corresponding thickness ratio is same for both theory and FEM. The occurrence of a peak is because, for low thickness ratios, the substrate is unable to effectively deform the PVDF layer and therefore reduce the charge sensitivity. At higher thickness ratios, most of the deformation is translated into uniform longitudinal strain and only a little bending of the beam takes place. The same is true in the case of elastic mismatch.[20] For the cases of lower bending stiffness (i.e., for small k_t and k_E values), the lateral stress T_2 and compressive stress T_3 are non-zero and significant.[21] Hence, FEM predicts a higher charge sensitivity value than theory and as the bending stiffness increase, the error diminishes. However, the optimal k_t and k_E values remain unchanged due to this effect. The effect is also reduced when the unimorph configuration is switched with PVDF layer at the bottom and the substrate at the top. The optimal k_t and k_E values are computed with the feasible region defined by the minimum bending stiffness values for the clamped-clamped and cantilever sensors.

Table 2 shows the optimized thickness ratio and elastic modulus ratio for the bending configurations. The charge sensitivity of cantilever sensor is three orders of magnitude higher than optimum compressive design and 3.15 times higher than the clamped-clamped configuration with segmented electrodes. The optimum elastic

modulus ratio is 8.11 same for both the configuration, whereas clamped-clamped design has a lower optimal thickness ratio for a given deflection sensitivity target. The response time of the sensor is directly related to the bandwidth and fundamental frequency of the sensor. For the surface pressure transducer to have a response time of 1 ms, it should have a minimum fundamental frequency of 350 Hz.[22] Assuming a mass density of 1200 kg m^{-3} (for typical polymers) and mass density of PVDF layer as 1880 kg m^{-3}, the fundamental frequency of the unimorphs is computed using FEM for the optimized structure. Table 2 shows that for the optimized k_t and k_E values, all the configurations meet the target fundamental frequency. PVDF sensor in compressive mode is the fastest design followed by the clamped-clamped configuration owing to their higher bending stiffnesses. Finally, the above pressure sensors connected to a conventional low frequency charge amplifier with feedback capacitance 1 nF is expected to provide a voltage sensitivity of 86 µV Pa^{-1} for the compressive design, 0.33 mV Pa^{-1} for the clamped-clamped design, and 1.04 mV Pa^{-1} for the cantilever design.[5]

Table 2: Optimized values for different configurations.

Configuration	**Optimum elastic modulus ratio** $k_{E,opt}$	**Optimum thickness ratio** $k_{t,opt}$	**Natural frequency** f_1 **[kHz]**	**Deflection sensitivity** δ_P $[\mu m$ **Pa**$^{-1}]$	**Charge sensitivity** Q_P **[pC Pa**$^{-1}]$		
					FEM	**Theory**	**Error (%)**
Compressive	-	-	171	0.0001	6.2 x 10^{-4}	8.6 x 10^{-4}	-39.1
Clamped-clamped	8.11	0.32	5.33	0.023	0.35	0.34	2.9
Cantilever	8.11	0.81	1.09	0.33	1.07	1.04	2.8

4. CONCLUDING REMARKS

This work utilized a generalized expression for deflection and polarization of piezoelectric bending unimorphs based on Euler-Bernoulli beam theory in order to arrive at deflection and charge sensitivity of PVDF pressure sensors. While operating below its first natural frequency, for maximum charge output, the cantilever configuration should have a uniform electrode coverage over the entire length of the PVDF layer, whereas the electrodes of the clamped-clamped configuration should be segmented in accordance with the stress distribution along the length of the sensor. A numerical study is performed to arrive at minimum bending stiffness values required in order to achieve a deflection sensitivity target of 0.5 μm Pa^{-1}. It is observed that the clamped-clamped unimorph meets the target for the investigated range of thickness and elastic modulus ratios of the substrate, whereas the cantilever has a minimum thickness ratio for a given elastic modulus. The analytical model for charge sensitivity agrees well with the FEM simulation with the error being higher for designs with lower bending stiffnesses due to d_{32} and d_{33} effect. There exists a non-monotonic dependence of thickness and elastic modulus ratio on the charge sensitivity. The charge sensitivity of the optimized cantilever sensor is three orders of magnitude greater than for compressive (d_{33}) mode and 3.15 times greater than the clamped-clamped configuration with segmented electrodes. The optimum elastic modulus ratio is 8.11 for both the bending unimorph configurations. The clamped-clamped design has an optimum thickness ratio of 0.32, whereas the cantilever design has a higher optimum thickness ratio of 0.81 due to its lower bending stiffness. Assuming typical polymer density for the substrate, all the optimized configurations meet the target natural frequency of 350 Hz with compressive sensor being the fastest design followed by the clamped-clamped configuration.

Acknowledgment

Financial support was provided by the member organizations of the Smart Vehicle Concepts Center, a Phase III National Science Foundation Industry-University Cooperative Research Center (www.SmartVehicleCenter.org) under grant NSF IIP 1738723. Technical advice was provided by Dr. Umesh Gandhi and Mr. Ryohei Tsuruta from Toyota Technical Center (TEMA-TTC) in Ann Arbor, MI.

REFERENCES

[1] T. Stathopoulos, I. Zisis, and E. Xypnitou, "Local and overall wind pressure and force coefficients for solar panels," *Journal of Wind Engineering and Industrial Aerodynamics* **125**, pp. 195–206, 2014.

[2] M. Gomes, A. Rodrigues, and P. Mendes, "Experimental and numerical study of wind pressures on irregular-plan shapes," *Journal of Wind Engineering and Industrial Aerodynamics* **93**(10), pp. 741–756, 2005.

[3] T. Yamashita, T. Makihara, K. Maeda, and K. Tadakuma, "Unsteady aerodynamic response of a vehicle by natural wind generator of a full-scale wind tunnel," *SAE International Journal of Passenger Cars-Mechanical Systems* **10**(2017-01-1549), pp. 358–368, 2017.

[4] Y. Le Sant and M. Merienne, "Surface pressure measurements by using pressure-sensitive paints," *Aerospace Science and Technology* **9**(4), pp. 285–299, 2005.

[5] J. Sirohi and I. Chopra, "Fundamental understanding of piezoelectric strain sensors," *Journal of intelligent material systems and structures* **11**(4), pp. 246–257, 2000.

[6] W. Nitsche, P. Mirow, and J. Szodruch, "Piezo-electric foils as a means of sensing unsteady surface forces," *Experiments in Fluids* **7**(2), pp. 111–118, 1989.

[7] W. Luber and J. Becker, "Application of pvdf foils for the measurements of unsteady pressures on wind tunnel models for the prediction of aircraft vibrations," in *Structural Dynamics, Volume 3*, pp. 1157–1176, Springer, 2011.

[8] C. Sullivan and T. Mueller, "Polyvinylidene fluoride film sensors for measurement of unsteady pressures on aerodynamic surfaces part i: Design, fabrication, calibration and demonstration," *Experiments in Fluids* **27**(1), pp. 79–84, 1999.

[9] Y. Wang, C. Huang, Y. Lee, and H. Tsai, "Development of a pvdf sensor array for measurement of the impulsive pressure generated by cavitation bubble collapse," *Experiments in Fluids* **41**(3), pp. 365–373, 2006.

[10] W. Zhu, C. Li, Y. Zhong, and P. Lin, "Re-design for automotive window seal considering high speed fluid-structure interaction," *SAE International Journal of Materials and Manufacturing* **10**(2), pp. 107–113, 2017.

[11] H. Takahashi, N. Dung, K. Matsumoto, and I. Shimoyama, "Differential pressure sensor using a piezoresistive cantilever," *Journal of Micromechanics and Microengineering* **22**(5), p. 055015, 2012.

[12] A. Batra, A. Alomari, M. Aggarwal, and A. Bandyopadhyay, "Energy harvesting under excitation of clamped-clamped beam," in *Smart Materials and Nondestructive Evaluation for Energy Systems 2016*, **9806**, p. 980612, International Society for Optics and Photonics, 2016.

[13] R. Kashyap, T. Lenka, and S. Baishya, "A model for doubly clamped piezoelectric energy harvesters with segmented electrodes," *IEEE Electron Device Letters* **36**(12), pp. 1369–1372, 2015.

[14] J. Smits and W. Choi, "The constituent equations of piezoelectric heterogeneous bimorphs," *IEEE Transactions on Ultrasonics, Ferroelectrics, and Frequency Control* **38**(3), pp. 256–270, 1991.

[15] Measurement Specialties, Inc., *Piezo Film Sensors Technical Manual*, 1999.

[16] J. Reddy, *Mechanics of laminated composite plates and shells: theory and analysis*, CRC press, 2004.

[17] S. Du, Y. Jia, S. Chen, C. Zhao, B. Sun, E. Arroyo, and A. Seshia, "A new electrode design method in piezoelectric vibration energy harvesters to maximize output power," *Sensors and Actuators A: Physical* **263**, pp. 693–701, 2017.

[18] M. Pillai, D. Ebenezer, and E. Deenadayalan, "Analytical model of mechanically excited piezoelectric unimorph beams," *The Journal of the Acoustical Society of America* **142**(2), pp. 718–727, 2017.

[19] Q. Wang, X. Du, B. Xu, and L. Cross, "Theoretical analysis of the sensor effect of cantilever piezoelectric benders," *Journal of Applied Physics* **85**(3), pp. 1702–1712, 1999.

[20] G. Gehring, M. Cooke, I. Gregory, W. Karl, and R. Watts, "Cantilever unified theory and optimization for sensors and actuators," *Smart Materials and Structures* **9**(6), p. 918, 2000.

[21] T. Ha, J. Zhang, and N. Lu, "Thickness ratio and d 33 effects on flexible piezoelectric unimorph energy conversion," *Smart Materials and Structures* **25**(3), p. 035037, 2016.

[22] W. Palm, *System dynamics*, McGraw-Hill Science, 2014.